

## All-Electron APW+*lo* calculation of magnetic molecules with the SIRIUS domain-specific package

Long Zhang,<sup>1,2,3</sup> Anton Kozhevnikov,<sup>4</sup> Thomas Schulthess,<sup>4</sup> S. B. Trickey,<sup>1,2,3</sup> and Hai-Ping Cheng<sup>1,2,3, a)</sup>

<sup>1)</sup>*Department of Physics, University of Florida, Gainesville, FL 32611, USA*

<sup>2)</sup>*Quantum Theory Project, University of Florida, Gainesville, FL 32611, USA*

<sup>3)</sup>*Center for Molecular Magnetic Quantum Materials, University of Florida, Gainesville, FL 32611, USA*

<sup>4)</sup>*Swiss National Supercomputing Centre, Zurich, Switzerland*

We report APW+*lo* (augmented plane wave plus local orbital) density functional theory (DFT) calculations of molecule systems using the domain specific SIRIUS multi-functional DFT package. Compared to other packages the additional APW and FLAPW task and data parallelism and the additional eigensystem solver provided by the SIRIUS package can be exploited for performance gains in in the ground state Kohn-Sham calculation. This is in contrast with the use of SIRIUS as a library backend to some other APW+*lo* or FLAPW (full-potential linearized AWP) code. We benchmark the code and demonstrate performance on several magnetic molecule and metal organic framework systems. We show that the SIRIUS package in itself is capable of handling systems as large as a few hundreds of atoms in the unit cell without losing the accuracy needed for magnetic systems.

---

<sup>a)</sup>Electronic mail: hping@ufl.edu

# I. INTRODUCTION

Molecular magnetism, including molecular magnetic materials, is a very active interdisciplinary research area that has significant implications for computational investigations. Motivated in no small measure by the promise of high impact on quantum computing<sup>1,2</sup>, molecular magnetism deals with design, synthesis, and physical and chemical characterization of both single-molecule magnets (SMMs)<sup>3,4</sup> and condensed aggregates thereof. Predictive and interpretive first principles calculations are valuable both for experimental progress and for formulation and parameterization of models of the molecular spin systems. We begin therefore with a brief overview of the physical problem class, then turn to attendant computational challenges and some progress in meeting them.

## A. Motivation from physical systems

Molecular magnetism involves a large range of dimensionality, from isolated SMMs<sup>5,6</sup> and 1D chain magnets<sup>7,8</sup> through 2D molecular layers<sup>9</sup> to 3D polymers and metal organic framework<sup>10,11</sup> materials that exhibit collective ordering of magnetic moments.

Research activity, both theoretical and experimental, has grown in recent decades with focus on (1) low dimensional materials (motivated by their potential application in high-density magnetic storage and nano-scale devices)<sup>12,13</sup> and (2) so-called functional materials<sup>5,12,14,15</sup> (because of their strong response to changing external conditions). Because molecular magnets have well-localized magnetic moments, they are a nearly perfect arena for investigation of intriguing phenomena and testing models. Unlike bulk magnetic materials, their quantum size effects suggest applications beyond conventional high-density information storage. Such applications include spintronics and qubits for quantum computing.

The molecules involved are large and rather complicated. An example category is Mn<sub>12</sub> complexes<sup>16</sup>. Their investigation dates to synthesis by Weinland and Fischer in 1921<sup>17</sup>. The crystal structure was not determined until 1980<sup>18</sup>. That particular Mn<sub>12</sub> molecule was built from four Mn<sub>4+</sub> ( $S = 3/2$ ) and eight Mn<sub>3+</sub> ( $S = 2$ ) ions coupled by oxygen atoms. The [Mn<sub>12</sub>O<sub>12</sub>(O<sub>2</sub>CPh)<sub>16</sub>(H<sub>2</sub>O)<sub>4</sub>] complex was studied beginning in 1988,<sup>19</sup> and its ground state eventually determined<sup>20,21</sup> to have  $S = 10$ . For computational context, note that this last system has 176 atoms and 1210 electrons.

A major class of experimental effort has focused on design and synthesis of multi-nuclear clusters containing<sup>4</sup>  $\text{Mn}^{3+}$ , because the axially Jahn-Teller distorted  $\text{Mn}^{3+}$  ions usually possess large magnetic anisotropy due to spin-orbital coupling. A large number of Mn(III)-based SMMs has been reported, including those with  $\text{Mn}_6$ <sup>22</sup>,  $\text{Mn}_{19}$ <sup>23-25</sup>,  $\text{Mn}_{25}$ <sup>26,27</sup>,  $\text{Mn}_{31}$ <sup>28</sup> and  $\text{Mn}_{84}$ <sup>29</sup>. In addition, inorganic chemists have also synthesized many transition metal (TM) SMMs based upon anisotropic  $\text{V}^{3+}$ ,  $\text{Fe}^{2+/3+}$ ,  $\text{Ni}^{2+}$ , and  $\text{Co}^{2+}$  ions; see Refs. 3, 30–35. The octa-nuclear cluster  $[\text{Fe}_8\text{O}_2(\text{OH})_{12}](\text{tacn})_6]^{8+}$  ( $\text{Fe}^8$ ) reported by Sangregorio et al.<sup>31</sup> is an example. It has 174 atoms and 756 electrons with an  $S = 10$  ground state that arises from competing anti-ferromagnetic interactions among eight  $\text{Fe}^{3+}$  ( $S = 5/2$ ) ions<sup>36</sup>. Magnetic measurements revealed that it has an anisotropy barrier of  $17 \text{ cm}^{-1}$ , much smaller than that of  $\text{Mn}_{12}$  complexes. Other significant synthesis effort has been focused on enhancing the magnetic anisotropy of the molecule<sup>37-40</sup>. That has stimulated the development of several different groups of SMMs, such as cyano-bridged SMMs<sup>41-43</sup>, Ln-based SMMs<sup>44-48</sup>, 3d-4f electron elements based SMMs<sup>46,49</sup>, actinide-based SMMs<sup>47</sup>, radical-bridged SMMs<sup>50</sup> and organo-metallic SMMs<sup>51</sup>.

The essential context for insightful computational studies illustrated by this brief overview is that SMMs are large, structurally and electronically intricate molecules with complicated spin manifolds. Materials comprised of them are more complicated and demanding. Many of the chemical details of SMMs are largely irrelevant at this stage. However, the presence of heavy nuclei and the importance of anisotropy both implicate the significance of relativistic effects, including spin-orbit coupling. Predictive, materials-specific simulations of systems composed from SMMs thus are extremely challenging.

## B. Predictive computational approaches

At present, density functional theory (DFT)<sup>52</sup> is the most widely used first-principles calculation method in material science. General DFT is based on the Hohenberg-Kohn theorems stating that every observable of an interacting electron system is a functional of its ground-state charge density, that minimizes the total energy of the system<sup>53</sup>. The theorems do not answer the question how to obtain such a ground-state density. A recipe for obtaining the ground state charge density is given by Walter Kohn and Lu Jeu Sham who introduce an auxiliary system of non-interacting particles<sup>54</sup>. The non-interacting particles, described

by the Schrodinger-like Kohn-Sham equations, share the same ground state charge density with the interacting particles. With a numerical basis, one can expand the wavefunctions, charge density and potential using the basis and convert the Kohn-Sham equations to a set of linear equations that can be solved using developed eigen system methods. Since the effective potential of the Kohn-Sham Hamiltonian depends on the charge density, which is not known for the true ground state, the Kohn-Sham equations are solved in an iterative procedure which requires the calculation of the density and the potential based on the updated wavefunctions in each iteration.

The all electron full potential linearized augmented plane wave (FLAPW) method is one flavor of implementation of the Kohn-Sham DFT. The method is based on a partitioning of the material's unit cell into non-overlapping muffin-tin (MT) spheres, centered at the atomic nuclei, and an interstitial (IS) region between the MT spheres, as illustrated in Fig. 1.

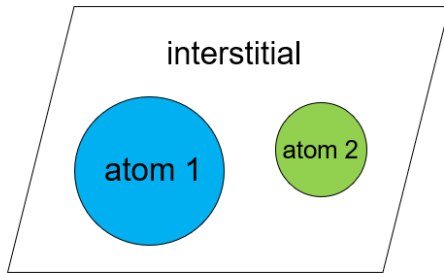


FIG. 1. Muffin-tin partitioning of a unit cell.

This method originated from the APW method proposed by Slater<sup>55,56</sup>. It brought great progress with the idea of linear methods<sup>57,58</sup> introduced by Andersen and applied by Koelling and Arbman using the model of muffin-tin shaped approximation to the potentials. The basis set is constructed according to the same space partition. One piece of the basis function for Bloch wave-vector  $\mathbf{k}$  and plane-wave vector  $\mathbf{G}$  is

$$\varphi_{\mathbf{k}}^{\mathbf{G}}(\mathbf{r}) = \begin{cases} \sum_{\ell, m} \sum_{\nu} A_{\ell m \nu}^{\alpha, \mathbf{k}}(\mathbf{G}) u_{\ell \nu}^{\alpha}(r) Y_{\ell m}(\hat{\mathbf{r}}), & \mathbf{r} \in \alpha \\ (1/\sqrt{\Omega}) e^{i(\mathbf{G}+\mathbf{k}) \cdot \mathbf{r}}, & \mathbf{r} \notin \alpha \end{cases}$$

Here  $u_{\ell \nu}^{\alpha}(r)$  is the solution of the (energy dependent) radial Schrodinger equation in the MT sphere labeled  $\alpha$ ;  $Y_{\ell m}(\hat{\mathbf{r}})$  are spherical harmonics;  $A_{\ell m \nu}^{\alpha, \mathbf{k}}(\mathbf{G})$  are the matching coefficients for connection with the interstitial plane wave;  $\ell$  and  $m$  are the azimuthal and magnetic

quantum numbers in a particular sphere; and  $\nu$  is the order of energy derivative of the radial function (the APW basis set does not have continuous radial first derivatives at the sphere boundaries.) The dependence of the radial functions upon the energy for which they are solved is the difficulty with the APW basis set. Continuity at sphere boundaries requires those solution energies to correspond to KS eigenvalues. That correspondence makes the KS secular equation highly non-linear in the one-electron energies. The problem is remedied by introducing the energy derivative of the radial function in the APW basis,  $\dot{u}_{\ell\nu}^\alpha = [\partial/\partial\epsilon]u_{\ell\nu}^\alpha$ , that makes the basis a linearized APW (LAPW) basis. The basis can be enhanced with additional local orbitals (*lo*), which are radial functions and energy derivatives, that vanish at the MT boundaries.

The electron density and the Kohn-Sham effective potential are expanded in correspondence to the space division in the unit cell. In the interstitial region they are expanded in plane waves and inside MT spheres in real spherical harmonics  $R_{\ell m}(\mathbf{r})$ :

$$n(\mathbf{r}) = \begin{cases} \sum_{\ell m} n_{\ell m}^\alpha(r) R_{\ell m}(\hat{\mathbf{r}}), & \mathbf{r} \in \alpha \\ \sum_{\mathbf{G}} \tilde{n}(\mathbf{G}) e^{i\mathbf{G}\cdot\mathbf{r}}, & \mathbf{r} \notin \alpha \end{cases} \quad (1)$$

and

$$v_{KS}(\mathbf{r}) = \begin{cases} \sum_{\ell m} v_{\ell m}^\alpha(r) R_{\ell m}(\hat{\mathbf{r}}), & \mathbf{r} \in \alpha \\ \sum_{\mathbf{G}} \tilde{v}(\mathbf{G}) e^{i\mathbf{G}\cdot\mathbf{r}}, & \mathbf{r} \notin \alpha . \end{cases} \quad (2)$$

Here  $n_{\ell m}^\alpha(r)$ ,  $\tilde{n}(\mathbf{G})$ ,  $v_{\ell m}^\alpha(r)$ , and  $\tilde{v}(\mathbf{G})$  are expansion coefficients determined through the self-consistent solution of the KS equation.

Due to the fact that it contains no shape approximation to the atomic potential and includes all electrons into consideration, FLAPW DFT is often considered as a highly precise realization of density functional theory and can be use as a gold standard to measure the precision of other approaches.

The present work focuses on the domain specific SIRIUS library package. Our goal is to make fast and efficient all-electron, full-potential DFT calculations routinely feasible for large and complicated systems such as magnetic molecules and their aggregates. In the following sections, we first describe the package and its intended usage for accelerating plane-wave based DFT codes. We then explain its value when used as a stand-alone FLAPW package.

After describing the library, we demonstrate its capabilities by calculations on a selection of magnetic molecules.

## II. THE SIRIUS PACKAGE

Irrespective of the particular code, LAPW/APW+LO/*lo* calculations obviously have the same underlying formalism. Because the basic conceptualization starts with plane waves, those codes also share significant formal and procedural elements with plane-wave pseudo-potential (PW-PP) codes. Specifically the following tasks are shared: unit cell setup, atomic configurations, definition and generation of reciprocal lattice vectors  $\mathbf{G}$  and combinations with Bloch wave vectors  $\mathbf{G} + \mathbf{k}$ , definition of basis functions on regular grids as Fourier expansion coefficients; construction of the plane wave contributions to the KS Hamiltonian matrix, generation of the charge density, effective potential, and magnetization on a regular grid; symmetrization operations on the charge density, potential and occupation matrix; iteration-to-iteration mixing schemes for density and potential; diagonalization of the secular equation. Compared to PW-PP codes, FLAPW/APW+*lo* additionally have everything expanded in radial functions and spherical harmonics inside the MT spheres, and enforcement of matching conditions on sphere surfaces.

From a development perspective, these commonalities offer an opportunity. Rather than have the developers of each individual code devise — and in many cases essentially reinvent — various schemes for computational speed and scalability, we can proceed via *separation of concerns*, identify the general calculation elements within the plane wave Kohn-Sham DFT formalism and create a library with explicit support for FLAPW/APW+*lo* and PW-PP calculations. By abstracting and encapsulating the common objects such as the examples just given, the focus then can be on optimizing computational performance. The SIRIUS library was created as such an optimized collection. It was designed from the outset with both task parallelization and data parallelization. It has been optimized for multiple MPI levels as well as OpenMP parallelization and also optimized for GPU utilization.

SIRIUS can be interfaced directly with both existing FLAPW/APW+*lo* codes and with PW-PP codes as a *DFT library*. We discuss that use of SIRIUS elsewhere<sup>59</sup>. Though that was the originally intended primary usage SIRIUS does have basic FLAPW/LAPW+*lo* stand-alone capability. The present study investigates its benefits to large-scale magnetic

system calculations in that form.

The SIRIUS package is written in C++ in combination with the CUDA<sup>60</sup> backend to provide the following features: (1) low-level support such as pointer arithmetic and type casting as well as high-level abstractions such as classes and template meta-programming; (2) easy interoperability between C++ and widely used Fortran90; (3) full support from the standard template library (STL)<sup>61</sup>; (4) easy integration with the CUDA nvcc compiler<sup>62</sup>. The SIRIUS code provides dedicated API functions to interface to QuantumEspresso and *exciting*.

Importantly for large-system calculations, SIRIUS is designed and implemented with both task distribution and data (large array) distribution in mind. Virtually all KS electronic structure calculations rely at minimum on two basic functionalities: distributed complex matrix-matrix multiplication (`pzgemm` in LAPACK) and a distributed generalized eigenvalue solver (`pzhgvx` also in LAPACK). SIRIUS handles these two major tasks with data distribution and multiple levels of task distribution.

The eigenvalue solver deserves scrutiny. Development of *exciting* revealed that considerable changes in code were required to scale the calculation to a larger number of distributed tasks, for example, by making the code switchable from LAPACK to ScaLAPACK. This can be seen by comparing the task distribution and data distribution of the base ground state subroutine in recent versions of *exciting* (version Nitrogen for example) and ELK (version 5.2.14 or earlier version for example). Evidently the ELK developer team had emphasized physics features and functionalities rather than adding support for ScaLAPACK. The situation is similar with Exciting-Plus<sup>63</sup>; it has only LAPACK support and does not have data distribution of large arrays.

Eigenvalue solver performance depends upon intrinsic limitations of the underlying algorithms. Widely used linear algebra libraries such as LAPACK and ScaLAPACK implement robust full diagonalization algorithms that can handle system size up to about  $10^6$ . But, unfortunately, because of the very large plane wave cutoff needed for FLAPW/APW+*lo* calculations on systems as large as 100+ atoms, the eigensystem often is several times larger than that. A Davidson-type<sup>64</sup> iterative diagonalization algorithm is often suitable for such large systems because it suffices to solve for the lowest 10–20 percent of all eigenvalues and the associated eigenvectors to obtain the valence band structure around the Fermi energy. But Davidson-type diagonalization algorithms are not offered in standard linear algebra

libraries. That omission is at least in part because such algorithms involve repeated application of the Hamiltonian to a sub-space of the system. Thus the algorithm depends on construction details of the Hamiltonian matrix, i.e. it depends on the specific DFT formalism. The SIRIUS library takes this into consideration and offers an efficient implementation of Davidson-type diagonalization<sup>65</sup> for FLAPW/APW+*lo* and PW-PP codes.

For computational capability, switching from LAPACK to ScaLAPACK gives the benefit of data parallelism but does not remove the diagonalization algorithm limitation. Switching from LAPACK (or ScaLAPACK) to a Davidson-type diagonalization addresses that. Doing so requires taking into consideration both the diagonalization algorithm and the handling of large data sets as the system size grows. This is especially so in the case of iterative diagonalization implemented in FLAPW/LAPW+*lo* basis codes. When the unit cell is as large as ten Å<sup>3</sup> and contains a hundred or more multi-electron atoms, the plane-wave cutoff needed is normally about 25–30  $a_0^{-1}$  to reach a properly converged ground state. This causes the reciprocal-lattice-vector ( $G$ -vector) related arrays to become very large. Again, the problem is illustrated by the ELK and *exciting* codes. Each has several multi-dimensional arrays that have one dimension for the global  $G$ -vector indices. Because those arrays are not handled in a distributed way, they become very memory consuming in a single MPI task. Eventually they become the real bottleneck, once the diagonalization algorithm limitation is removed via a Davidson-type method. Though designed originally for use as a library, SIRIUS, as written, treats the  $G$ -vector related multi-dimensional arrays in distributed manner from the beginning. And, it has basic FLAPW/LAPW+*lo* DFT ground state capability when running stand-alone. That makes SIRIUS stand-alone calculation much more suitable for large molecule systems. We turn to some examples.

### III. SIRIUS: [MN(TAA)] MOLECULE

The so-called [Mn(taa)] molecule ( $[Mn^{3+}(pyrol)_3(tren)]$ ) is a meridional pseudo-octahedral chelate complex of a single Mn as the magnetic center and the hexadentate tris[(E)-1-(2-azolyl)-2-azabut-1-en-4-yl]amine ligand. It is a spin-crossover system of long-standing interest. Originally studied by Sim and Sinn<sup>66</sup>, it was the first known example of a manganese(III)  $d^4$  spin-crossover system. Experimentally it is found that the  $Mn^{3+}$  cation goes from a low-spin state to a high-spin state (HS) at a transition temperature of about 45 K.

The [Mn(taa)] structure is sufficiently large that it has non-negligible intra-molecular dispersion interactions with a critical HS-LS difference. The HS state involves anti-bonding molecular orbital occupation, hence the octahedral HS complex tends to have weaker and longer metal-ligand bonds than the LS bonds. Therefore, the dispersion contribution to the metal-ligand bonding is lower for the HS case than for the more compact LS state. Mn(taa) poses challenges to the computational determination of the ground state because the purely molecular (non-thermal)  $\Delta E_{HL} = E_{HS} - E_{LS}$  is very small compared to the total energies. Estimates are about  $50 \pm 30$  meV but as high as a few hundred meV. Note that usual XC density functional approximations, suffer from a self-interaction error and hence tend to favor the LS state to reduce spurious self-repulsion with the result of overestimated  $\Delta E_{HL}$  values<sup>7</sup>. That is not of concern here since what we are testing is algorithmic efficiency.

Several factors can affect a DFT calculation of  $\Delta E_{HL}$  of the molecule significantly. For consistency with condensed phase calculations, it is appropriate to study the isolated molecule in a large, periodically bounded box. To ensure accuracy, the plane wave cutoff needs to be large. To treat the isolated molecule, the vacuum volume in the computational unit cell requires even larger cutoffs. This makes the APW+*lo* calculation an intensive job because of the large Hamiltonian to be diagonalized and the large  $G$ -vector related arrays.

The quality of APW+*lo* calculation is governed by the dimensionless quantity  $R_{min}^{MT} \cdot |\mathbf{G}^k|_{max}$ , where  $R_{min}^{MT}$  is the minimum muffin-tin radius of all atomic species and  $|\mathbf{G}^k|_{max}$  is the maximum length of the  $\mathbf{G} + \mathbf{k}$  vectors. The standard value of  $R_{min}^{MT} \cdot |\mathbf{G}^k|_{max}$  is 7 in most FLAPW codes, and can be 10 if one wants to push the accuracy of total energy to be close to  $\mu$ Ha. For organic molecules, the smallest  $R^{MT}$  is normally around  $1.4 a_0$  of the hydrogen atom, which makes  $|\mathbf{G}^k|_{max} \in [5, 7] a_0^{-1}$ . The size of the Hamiltonian in the first variational step is determined by  $|\mathbf{G}^k|_{max}$ , the total number of atoms and the local orbitals added to each atom.

For the Mn-taa molecule, if one sets  $R_{min}^{MT} \cdot |\mathbf{G}^k|_{max} = 7$  and other parameters as shown in Table.II, the size of the first variational Hamiltonian is about 330,000. This is actually within the theoretical limit of the LAPACK's full diagonalization algorithm. However, in order to run the DFT calculation, not only the  $\mathbf{G}^k$  vectors but also the  $\mathbf{G}$  vectors for expanding density and potential have to be handled efficiently. For molecules in a large cube unit cell of the size of  $20 \text{ \AA}$  with irregular vacuum space, we found (from SIRIUS calculation) that the  $|\mathbf{G}|$  for density and potential needs to be as large as  $25\text{--}30 a_0^{-1}$  to make the total energy

$ \mathbf{G} _{max} (a_0^{-1})$	20	25	30	35
peak memory (GB)	39.5	110.8	151.8	209.5

TABLE I. Peak memory consumption of single  $k$ -point Mn-taa calculation in a cube unit cell of 20 Å. Other input parameters are same as Table.II.

converge. If the arrays containing  $\mathbf{G}$  vector indices are not stored in a distributed way during the calculation, they become the major memory consuming quantities and make the calculation very slow. We have tried to use community codes like ELK and Exciting-Plus to calculate the ground state of Mn-taa and found it to be practically difficult. If one performs single  $k$ -point calculation for an isolated system, the lack of band parallelism within a  $k$ -point makes it run with one MPI task only. The desired large  $|\mathbf{G}|$  cutoff for density and potential requires a significant amount of memory that makes the calculation slow. A test to run the Mn-taa system using Exciting-Plus on NERSC Cori (128GB memory per node) found, when  $|\mathbf{G}| = 30 a_0^{-1}$  or larger, the calculation crashed with out-of-memory (OOM) error, even if one node was assigned with only one MPI task. To have a more specific measure of the memory issue we ran it on the UF HPC large memory node and observed the peak memory consumption values as shown in Table-I.

For the Sirius calculation of Mn-taa, we used the experimentally determined low spin [Mn(taa)] structures and the PBE<sup>67</sup> XC generalized gradient approximation (GGA). We set  $R_{min}^{MT} \cdot |\mathbf{G}^k|_{max} = 5$ ,  $|\mathbf{G}|_{max} = 30 a_0^{-1}$ , and other input parameter values listed in Table-II. There was no Hubbard  $U$ . The same structures and XC were used in a VASP<sup>68</sup> calculation for comparing the results, also in Table-II.

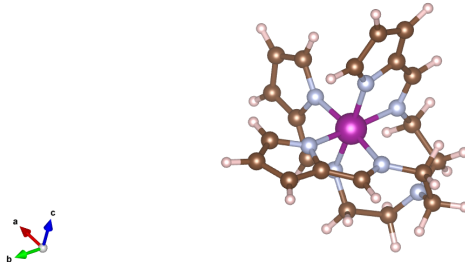


FIG. 2. Mn-taa molecule

TABLE II. Input parameters for the [Mn(taa)] LS state

structure	Mn-taa, LS state structure
unit cell	$20 \times 20 \times 20 \text{ \AA}$ box
number of atoms	55
$R_{mt} (a_0)$	Mn: 2.2; O: 1.6; C: 1.4; H: 1.0;
$R_{min}^{MT} \cdot  \mathbf{G}^k _{max}$	5
$ \mathbf{G}_{max}  (a_0^{-1})$ for $\rho$ and $V_{eff}$	30
$l_{max}$ for APW	8
$l_{max}$ for $\rho$ and $V_{eff}$	8
size of 1st variational Hamiltonian	$\approx 155,000$
$k$ -point grid	$1 \times 1 \times 1$
(L)APW configuration	$\epsilon_l = -0.15 \text{ eV}$ ; $\partial_E = 0$ ;
$lo$ configuration	Mn: $s, p, d$ ; O/C: $s, p$ ; H: $s$ ;
treated as core state	Mn: 1s, 2s, 2p, 3s; O/C: 1s
total energy tolerance	$10^{-6}$ Har
potential tolerance	$10^{-7}$ Har
run job setup:	16 MPI tasks 16 OMP threads per task
number of SCF iterations	35
average time per SCF iteration	55 s
HUMO-LOMO gap (eV)	0.68 (VASP: 0.66)
$\mu_{tot} (\mu_B)$	total: 2.00 (VASP: 2.00) Mn atom: 1.68 (VASP: 1.77)

#### IV. SIRIUS: $[\text{Mn}_3]_2$ MOLECULE

One highly desirable property for potential application to SMMs would be to demonstrate quantum mechanical coupling of two or more SMMs to one other or to a surface or other device component, all the while retaining their isolated-molecule magnetic properties to a useful degree. For this, an SMM-SMM coupled structure was identified for hydrogen-bonded supramolecular pairs of  $S = 9/2$  SMMs  $[\text{Mn}_4\text{O}_3\text{Cl}_4(\text{O}_2\text{CEt})_3(\text{py})_3]^{69-71}$ . Since hydrogen-bonded inter-SMM interactions do not provide easy control of oligomerization nor guarantee retention of the oligomeric structure in solution, covalently organic linked SMM-SMM structures were developed.

First along that line apparently was the  $[\text{Mn}_3]_4$  SMM tetramer<sup>72</sup>, which is covalently linked with dioximate linker groups. A recent further development is the  $[\text{Mn}_3]_2$  dimer molecule<sup>73</sup>. It is comprised of two  $\text{Mn}_3$  units covalently joined via dpd2-dioximate linkers. The two triangular  $\text{Mn}_3$  units are parallel, with each having the magnetic  $S = 6$  ground state from intra- $\text{Mn}_3$  ferromagnetic couplings. The inter- $\text{Mn}_3$  interaction also has been determined to be ferromagnetic. There is no experimental evidence for noticeable interactions between the two dimers. That is consistent with the absence of significant inter-dimer contacts in the structure and the relatively large distance between Mn ions in adjacent dimers. The interaction quantum mechanically couples the two  $\text{Mn}_3$  units. The structure is robust and resists any significant deformation or distortion that might affect the weak inter- $\text{Mn}_3$  coupling.

With 137 atoms and 748 electrons the  $[\text{Mn}_3]_2$  SMM dimer is the largest isolated molecule system we have treated with all-electron DFT calculations. Like the Mn-*taa*, this calculation also benefits from the band parallelization within a single  $k$ -point and the distributed storage of the  $G$ -vector related arrays. The molecule is also placed in a 20 Å periodically bounded box with single  $\mathbf{k}$ -point Brillouin Zone sampling. The  $G_{max}$  cutoff and LO/*lo* configuration for the Mn atoms were the same as for [Mn(*taa*)]. Also as before, we used the experimental geometry<sup>73</sup> and the PBE exchange-correlation functional<sup>67</sup> (again, no Hubbard  $U$ ). We are able to converge the system to the anti-ferromagnetic ground state, where there are two spin-up Mn and one spin-down Mn in each  $[\text{Mn}_3]$ , and the total moment is zero.

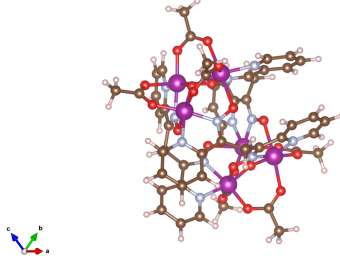


FIG. 3. Mn3 dimer molecule

TABLE III. Input parameters and outputs of Mn<sub>3</sub> dimer

	Mn <sub>3</sub> dimer
unit cell	$20 \times 20 \times 20 \text{ \AA}$ cubic
number of atoms in unit cell	137
$R_{mt} (a_0)$	Mn: 2.2; O/N: 1.4; C: 1.2; H: 1.0;
$R_{min}^{MT} \cdot  \mathbf{G}^k _{max}$	5
$ \mathbf{G}_{max}  (a_0^{-1})$ for $\rho$ and $V_{eff}$	30
$l_{max}$ for APW	8
$l_{max}$ for $\rho$ and $V_{eff}$	8
size of 1st variational Hamiltonian	$\approx 187,000$
$k$ -point grid	$1 \times 1 \times 1$
(L)APW configuration	$\epsilon_l = -0.15 \text{ eV}; \partial_E = 0;$
$lo$ configuration $\star$	Mn: $s, p, d$ ; O/C/N: $s, p$ ; H: $s$
core state	Mn: 1s, 2s, 2p, 3s; O/C/N: 1s
total energy tolerance	$10^{-6}$ Har
potential tolerance	$10^{-7}$ Har
run job setup:	16 MPI tasks 16 OMP threads per task
number of SCF iterations	125
average time per SCF iteration	$\approx 250$ s
HUMO-LOMO gap (eV)	0.23 (VASP: 0.27)
$\mu_{tot} (\mu_B)$	each Mn atom (Sirius): $\pm 1.88$ each Mn atom (Vasp): $\pm 1.95$

## V. SIRIUS: DTN MOLECULE

The insulating organic compound  $XCl_2-[SC(NH_2)_2]_4$  where  $X=Ni$  or  $Co$  (DTN and DTC molecules, respectively) is a molecule-based framework structure in which magnetic and electric order can couple with each other. It has been experimentally studied for its quantum magnetism<sup>74-77</sup>. ( $NiCl_2-[SC(NH_2)_2]_4$ ) has a tetragonal molecular crystal structure with two Ni atoms as magnetic centers in one unit cell. Each Ni has four S atoms and two Cl atoms as nearest neighbors, as shown in Fig. 4. Thus it forms an octahedral structure similar to the  $BO_6$  octahedra in  $ABO_3$  perovskites. The base octahedral structures pack in a body-centered tetragonal structure, with Ni-Cl-Cl-Ni bonding along the  $c$ -axis and hydrogen bonding between thiourea molecules in the  $a$ - $b$ -plane. The four thiourea  $[SC(NH_2)_2]$  molecules around each Ni ion are electrically polar. The  $a$ - $b$ -plane components of the thiourea electric polarization cancel, while the  $c$ -axis components are in the same direction, thereby creating a net  $c$ -axis electric polarization that could be responsible for magnetic field-modified ferroelectricity.

At temperatures below 1.2K and below a critical magnetic field, DTN is a quantum paramagnet. As the magnetic field perpendicular to the  $a$ - $b$ -plane reaches the first critical value, DTN experiences a quantum phase transition into an XY-antiferromagnetic state in which all Ni spins lie within the  $a$ - $b$ -plane. When the field is increased further the spins begin to be more aligned with a corresponding increase in magnetization. When a second critical field is reached, the magnetization saturates and the material enters a spin-polarized state with all spins aligned along the  $c$ -axis and parallel to the applied magnetic field.

There are three non-equivalent Ni-Ni spin couplings in the tetragonal DTN bulk:  $J_c$  along the  $c$ -axis (along the Ni-Cl-Cl-Ni bonding),  $J_{ab}$  in the  $a$ - $b$ -plane (nearest neighbors in that plane), and  $J_{diag}$  between the corner Ni at corner and the one at the tetragonal body center. Experiments suggest that the exchange coupling along the  $c$ -axis via the Ni-Cl-Cl-Ni chain is strong<sup>78</sup>, about about an order of magnitude larger than the other two Ni-Ni couplings. The system can behave as a quasi one-dimensional AFM with  $S = 1$  chains of  $Ni^{2+}$  ions. Recent DFT+ $U$  study<sup>79</sup> has shown that rather large Hubbard  $U$  correction (about 5-6 eV, relative to GGA-PBE XC approximation) is needed to match experimentally fit coupling constant values.

However the main qualitative physical feature, that  $J_c$  is about an order of magnitude

	$J_c$ (meV)	$J_{ab}$ (meV)	$J_{diag}$ (meV)
SIRIUS (DTN)	-2.72	-0.34	0.00
VASP (DTN) <sup>79</sup>	-1.05	-0.15	0.03

TABLE IV. Exchange coupling constants from Sirius calculation compared to VASP results.<sup>79</sup>

larger than  $J_{ab}$ , is already captured without Hubbard  $U$  correction in the DFT calculation. Therefore, we calculated the  $J$  constants without  $U$  using APW+ $lo$  as implemented in SIRIUS. To estimate the  $J$  values, one calculates the energy of the ferromagnetically and anti-ferromagnetically ordered state energies  $E_{FM}$  and  $E_{AFM}$  respectively.<sup>80</sup>. Then, assuming a Heisenberg Hamiltonian of the form  $H = J[S_1 \cdot S_2]$ , one can determine  $J$  from  $E_{FM} - E_{AFM}$ . The calculation involves creating two supercells,  $1 \times 1 \times 2$  for  $J_c$  and  $2 \times 1 \times 1$  for  $J_{ab}$ . The  $J_{diag}$  value can be obtained with the primitive unit cell. The supercells contain a number of atoms similar to that for the  $Mn_3$ -dimer molecule in the preceding example, namely 140 atoms and 888 electrons. Though the supercell is smaller by half (approximately  $10 \times 10 \times 20 \text{ \AA}^3$ ) than that needed for the Mn-*taa*, we found proper convergence in total energy still requires the PW cutoff magnitude for density and potential to be as large as  $|G_{max}|=30 (a_0^{-1})$ .

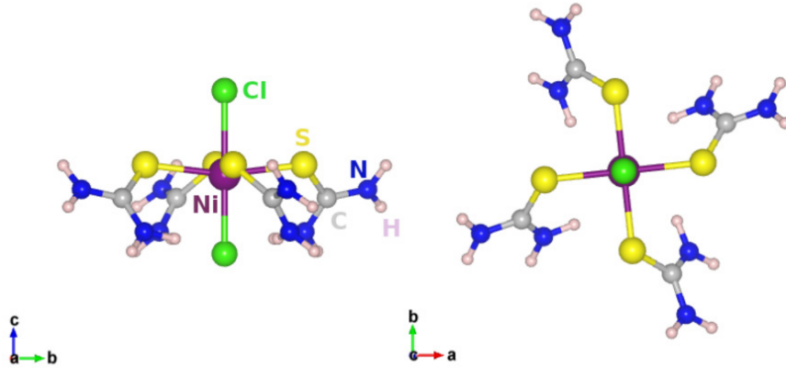


FIG. 4. base octahedral unit of DTN molecule<sup>79</sup>

TABLE V. Input parameters and outputs of DTN

	DTN $1 \times 1 \times 2$ supercell
unit cell	$\approx 10 \times 10 \times 20 \text{ \AA}$ box
number of atoms in unit cell	140
$R_{mt}$ ( $a_0$ )	Na/Co: 2.2; Cl/S/N: 1.4; C: 1.2; H: 1.2;
$R_{min}^{MT} \cdot  \mathbf{G}^k _{max}$	6
$ \mathbf{G}_{max} $ ( $a_0^{-1}$ ) for $\rho$ and $V_{eff}$	30
$l_{max}$ for APW	8
$l_{max}$ for $\rho$ and $V_{eff}$	8
size of 1st variational Hamiltonian	$\approx 225,000$
$k$ -point grid	$2 \times 2 \times 2$
(L)APW configuration for $l \leq l_{max}^{APW}$	$\epsilon_l = -0.15 \text{ eV}$ ; $\partial_E = 0$ ;
$lo$ configuration	Na/Co: $s, p, d$ Cl/S/C/N: $s, p$ ; H: $s$
treated as core state	Ni/Co: $1s, 2s, 2p, 3s$ Cl/S/C/N: $1s$
total energy tolerance	$10^{-7}$ Har
potential tolerance	$10^{-7}$ Har
run job setup:	64 MPI tasks 16 OMP threads per task
number of SCF iterations	90
average time per SCF iteration	$\approx 450 \text{ s}$
HUMO-LOMO gap (eV)	0.16 (VASP: 0.18)
magnetic moment	Ni atom: $\pm 0.75$ (VASP: $\pm 0.82$ )

## VI. SIRIUS: $[\text{Fe}(t\text{Bu}_2\text{qsal})_2]$ MOLECULE

The  $[\text{Fe}(t\text{Bu}_2\text{qsal})_2]$  molecule is a newly created spin crossover system<sup>81</sup>. Here (*tBu*<sub>2</sub>*qsal*) stands for 2,4-diterbutyl-6-((quinoline-8-ylimino)methyl)phenolate. The crystallized structure was determined by X-ray diffraction to be monoclinic, space group  $P2_1/c$ . It is potentially a functional molecule magnets material because  $[\text{Fe}(t\text{Bu}_2\text{qsal})_2]$  can be sublimed at 473–573 K and  $10^{-3}$ – $10^{-4}$  mbar, hence its thin-film deposition on a substrate is possible. The system undergoes a hysteretic spin transition. The average Fe–N and Fe–O bond lengths elongate from 1.949(2) Å at 100 K to 2.167(2) Å at 230 K and from 1.945(1) Å at 100 K to 1.997(1) Å at 230 K, respectively. These changes indicate that a conversion from the LS ( $S = 0$ ) to HS ( $S = 2$ ) structure takes place as the temperature is increased. In addition, pseudo-potential based DFT calculations<sup>82</sup> found the electron transfer is minimal for the molecule on a monolayer of Au(111) that suggests very small changes in the electronic structure and magnetic properties.

For this size of the system (436 atoms, 2435 electrons), we used  $R_{min}^{MT} \cdot G_{max} = 5$  and similar other cutoffs as used for previous systems. The large number of atoms does not make the Hamiltonian significantly larger but costs much more time in each iteration. With the cutoff parameters listed in VI we managed to converge the system to a non-magnetic ground state.

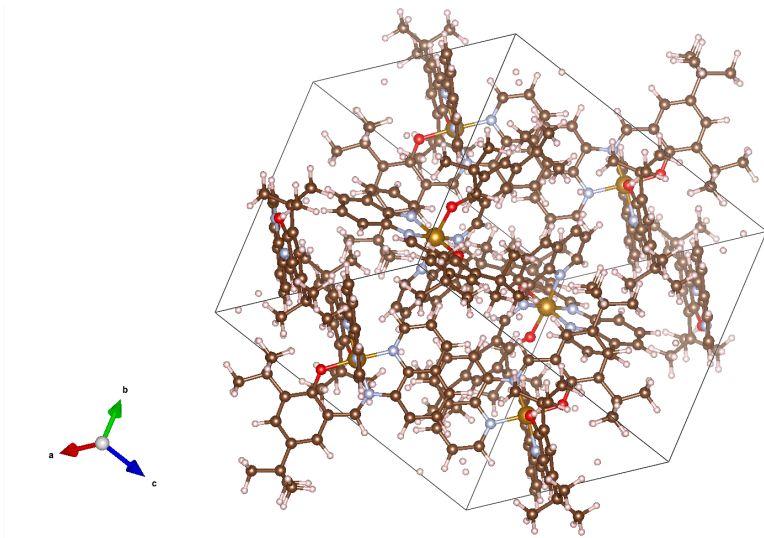


FIG. 5. the Fe4 molecule

TABLE VI. Input parameters of Fe<sub>4</sub> molecule, S=0

	Fe <sub>4</sub> MOF
unit cell	$15 \times 16 \times 17.5 \text{ \AA}$
number of atoms in unit cell	430
$R_{mt} (a_0)$	Fe: 2.2; O: 1.4; C: 1.2; H: 1.0;
$R_{min}^{MT} \cdot  \mathbf{G}^k _{\max}$	5
$ \mathbf{G}_{max}  (a_0^{-1})$ for $\rho$ and $V_{\text{eff}}$	30
$l_{\max}$ for APW	8
$l_{\max}$ for $\rho$ and $V_{\text{eff}}$	8
size of 1st variational Hamiltonian	$\approx 325,000$
$k$ -point grid	$1 \times 1 \times 1$
(L)APW configuration	$\epsilon_t = -0.15 \text{ eV}; \partial_E = 0;$
$lo$ configuration $\star$	Fe: $s, p, d$ Cl/S/C/N: $s, p$ ; H: $s$
treated as core state	Ni/Co: $1s, 2s, 2p, 3s$ Cl/S/C/N: $1s$
total energy tolerance	$10^{-6} \text{ Har}$
potential tolerance	$10^{-7} \text{ Har}$
run job setup:	64 MPI tasks 16 OMP threads per task
number of SCF iterations	135
average time per SCF iteration	$\approx 1400 \text{ s}$
HUMO-LOMO gap (eV)	0.0 (VASP: 0.0)

## VII. SUMMARY AND CONCLUSION

The main outcome of this work is to demonstrate, by several concrete examples, the value of the SIRIUS architecture and implementation for all-electron DFT calculations on fairly large molecules with complicated spin manifolds. By inference, this capacity extends to aggregates of such systems. SIRIUS as a stand-alone package provides performance gains through refined diagonalization methods and task and data parallelization improvements. The result is an advance in capability of the FLAPW-APW+*lo* DFT treatment of complex molecular aggregates.

In detail, the eigenvalue solver and the distribution of  $G$ -vector arrays in community FLAPW codes, for example ELK, *exciting* and Exciting-Plus are major bottleneck in calculations of large systems. The LAPACK/ScaLAPACK full diagonalization algorithm cannot handle Hamiltonian matrices larger than  $\sim 10^6$ , and the  $G$ -vector arrays cannot be efficiently handled without distributed storage. The SIRIUS package provides better data distribution and options to the use of the various (LAPACK, ScaLAPACK, Davidson) diagonalization algorithms. One can easily perform Davidson-type diagonalization of the Hamiltonian in the self-consistent loop and benefit from multiple MPI and thread-level parallelization within  $k$ -points and within bands. Together with the proper distribution of  $G$ -vector related arrays, the SIRIUS package can do plane wave based LAPW and APW+*lo* calculation of systems larger than many community LAPW/APW+*lo* codes.

We showed results from molecules using the APW+*lo* basis. The resulting total energy and magnetization are in agreement with experimental measurements and corresponding VASP calculations. In these test calculations, good scaling in band parallelization is observed, which is particularly crucial for a single  $k$ -point calculations ([Mn(*taa*)], Mn<sub>3</sub> dimer). The results also indicate that SIRIUS parallelization works well on contemporary high performance systems and the computational time is drastically reduced compared to ELK and Exciting-Plus for example. For a system of the size of DTN supercell studied in this work, the main physical feature is captured by extraction of exchange constants  $J$  from the total energies. The results are qualitatively in agreement with experiment and VASP calculations.

Looking ahead, all-electron FLAPW and APW+*lo* calculations of medium to large molecule and MOF systems is a relatively little-explored area. It is plausible that important core effects from, for example, spin-orbit coupling will be uncovered by such all-electron

investigations. At the least, the use of plane-wave-PAW codes to drive ab initio BOMD will be validated at sample configurations by such all-electron calculations. We have shown that the SIRIUS package can handle systems as large as 200 non-H atoms routinely without losing the accuracy needed for magnetic systems. With suitable high-performance systems, SIRIUS demonstrably can be used for systems up to 430 atoms and, we surmise, larger.

**Acknowledgment** This work was supported as part of the Center for Molecular Magnetic Quantum Materials, an Energy Frontier Research Center funded by the U.S. Department of Energy, Office of Science, Basic Energy Sciences under Award No. DE-SC0019330. Computations were performed at NERSC and the University of Florida Research Computer Center.

## REFERENCES

- <sup>1</sup>M. R. Wasielewski, M. D. E. Forbes, N. L. Frank, K. Kowalski, G. D. Scholes, J. Yuen-Zhou, D. E. F. Marc A. Baldo, R. H. Goldsmith, T. G. III, M. L. Kirk, J. K. McCusker, J. P. Ogilvie, D. A. Shultz, S. Stoll, and K. B. Whaley, “Exploiting chemistry and molecular systems for quantum information science,” *Nature Reviews Chemistry* **4**, 490–504 (2020).
- <sup>2</sup>A. Gaita-Ariño, F. Luis, s. Hill, and E. Coronado, “Molecular spins for quantum computation,” *Nature Chemistry* **11**, 301–309 (2019).
- <sup>3</sup>S. L. Castro, Z. Sun, C. M. Grant, J. C. Bollinger, D. N. Hendrickson, and G. Christou, “Single-molecule magnets: Tetranuclear vanadium(iii) complexes with a butterfly structure and an  $s = 3$  ground state,” *Journal of the American Chemical Society* **120**, 2365–2375 (1998), <https://doi.org/10.1021/ja9732439>.
- <sup>4</sup>R. Bagai and G. Christou, “The drosophila of single-molecule magnetism: [mn12o12(o2cr)16(h2o)4],” *Chem. Soc. Rev.* **38**, 1011–1026 (2009).
- <sup>5</sup>C. Marrows, L. Chapon, and S. Langridge, “Spintronics and functional materials,” *Materials Today* **12**, 70–77 (2009).
- <sup>6</sup>J. R. Friedman and M. P. Sarachik, “Single molecule nanomagnets,” *Annual Review of Condensed Matter Physics* **1**, 109–128 (2010), <https://doi.org/10.1146/annurev-conmatphys-070909-104053>.
- <sup>7</sup>P. L. Feng and D. N. Hendrickson, “Isostructural single-chain and single-molecule magnets,” *Inorganic Chemistry* **49**, 6393–6395 (2010), PMID: 20565068, <https://doi.org/10.1021/ic101016t>.
- <sup>8</sup>J. L. Rong-Min Wei, Fan Cao, “Single-chain magnets based on octacyanotungstate with the highest energy barriers for cyanide compounds,” *Scientific Reports* **6** (2016), 10.1038/srep24372.
- <sup>9</sup>L.-M. Zheng, J. Tang, H.-L. Sun, and M. Ren, “Low dimensional molecular magnets and spintronics,” in *Handbook of Spintronics*, edited by Y. Xu, D. D. Awschalom, and J. Nitta (Springer Netherlands, Dordrecht, 2016) pp. 617–680.
- <sup>10</sup>A. E. Thorarinsdottir and T. D. Harris, “Metal–organic framework magnets,” *Chemical Reviews* **120**, 8716–8789 (2020), PMID: 32045215, <https://doi.org/10.1021/acs.chemrev.9b00666>.
- <sup>11</sup>M. Kurmoo, “Magnetic metal–organic frameworks,” *Chem. Soc. Rev.* **38**, 1353–1379

- (2009).
- <sup>12</sup>W. W. Lapo Bogani, “Molecular spintronics using single-molecule magnets,” *Nature Materials* **7**, 179–186 (2008).
- <sup>13</sup>J. Gómez-Segura, J. Veciana, and D. Ruiz-Molina, “Advances on the nanostructuring of magnetic molecules on surfaces: the case of single-molecule magnets (smm),” *Chem. Commun.* , 3699–3707 (2007).
- <sup>14</sup>G. Mínguez Espallargas and E. Coronado, “Magnetic functionalities in mofs: from the framework to the pore,” *Chem. Soc. Rev.* **47**, 533–557 (2018).
- <sup>15</sup>J. M. Frost, K. L. M. Harriman, and M. Murugesu, “The rise of 3-d single-ion magnets in molecular magnetism: towards materials from molecules?” *Chem. Sci.* **7**, 2470–2491 (2016).
- <sup>16</sup>K. Ziemelis, “The difficult middle ground,” *Nature Physics* **4**, S19 (2008).
- <sup>17</sup>R. F. Weinland and G. Fischer, “Über manganiacetate und -benzoate,” *Zeitschrift für anorganische und allgemeine Chemie* **120**, 161–180 (1921), <https://onlinelibrary.wiley.com/doi/pdf/10.1002/zaac.19211200116>.
- <sup>18</sup>T. Lis, “Preparation, structure, and magnetic properties of a dodecanuclear mixed-valence manganese carboxylate,” *Acta Crystallographica Section B* **36**, 2042–2046 (1980), <https://onlinelibrary.wiley.com/doi/pdf/10.1107/S0567740880007893>.
- <sup>19</sup>P. D. W. Boyd, Q. Li, J. B. Vincent, K. Folting, H. R. Chang, W. E. Streib, J. C. Huffman, G. Christou, and D. N. Hendrickson, “Potential building blocks for molecular ferromagnets: [mn12o12(o2cph)16(h2o)4] with a  $s = 14$  ground state,” *Journal of the American Chemical Society* **110**, 8537–8539 (1988), <https://doi.org/10.1021/ja00233a036>.
- <sup>20</sup>A. Caneschi, D. Gatteschi, R. Sessoli, A. L. Barra, L. C. Brunel, and M. Guillot, “Alternating current susceptibility, high field magnetization, and millimeter band epr evidence for a ground  $s = 10$  state in [mn12o12(ch3coo)16(h2o)4].2ch3cooh.4h2o,” *Journal of the American Chemical Society* **113**, 5873–5874 (1991), <https://doi.org/10.1021/ja00015a057>.
- <sup>21</sup>R. Sessoli, H. L. Tsai, A. R. Schake, S. Wang, J. B. Vincent, K. Folting, D. Gatteschi, G. Christou, and D. N. Hendrickson, “High-spin molecules: [mn12o12(o2cr)16(h2o)4],” *Journal of the American Chemical Society* **115**, 1804–1816 (1993), <https://doi.org/10.1021/ja00058a027>.
- <sup>22</sup>E. Cremades, J. Cano, E. Ruiz, G. Rajaraman, C. J. Milios, and E. K. Brechin, “Theoretical methods enlighten magnetic properties of a family of mn6 single-

- molecule magnets,” *Inorganic Chemistry* **48**, 8012–8019 (2009), pMID: 19624160, <https://doi.org/10.1021/ic900992r>.
- <sup>23</sup>E. Ruiz, T. Cauchy, J. Cano, R. Costa, J. Tercero, and S. Alvarez, “Magnetic structure of the large-spin mn10 and mn19 complexes: A theoretical complement to an experimental milestone,” *Journal of the American Chemical Society* **130**, 7420–7426 (2008), pMID: 18489093, <https://doi.org/10.1021/ja800092s>.
- <sup>24</sup>O. Waldmann, A. M. Ako, H. U. Güdel, and A. K. Powell, “Assessment of the anisotropy in the molecule mn19 with a high-spin ground state  $s = 83/2$  by 35 ghz electron paramagnetic resonance,” *Inorganic Chemistry* **47**, 3486–3488 (2008), pMID: 18393411, <https://doi.org/10.1021/ic800213w>.
- <sup>25</sup>E. E. Moushi, T. C. Stamatatos, W. Wernsdorfer, V. Nastopoulos, G. Christou, and A. J. Tasiopoulos, “A family of 3d coordination polymers composed of mn19 magnetic units,” *Angewandte Chemie International Edition* **45**, 7722–7725 (2006), <https://onlinelibrary.wiley.com/doi/pdf/10.1002/anie.200603498>.
- <sup>26</sup>M. Murugesu, S. Takahashi, A. Wilson, K. A. Abboud, W. Wernsdorfer, S. Hill, and G. Christou, “Large mn25 single-molecule magnet with spin  $s = 51/2$ : Magnetic and high-frequency electron paramagnetic resonance spectroscopic characterization of a giant spin state,” *Inorganic Chemistry* **47**, 9459–9470 (2008), pMID: 18788733, <https://doi.org/10.1021/ic801142p>.
- <sup>27</sup>M. Murugesu, M. Habrych, W. Wernsdorfer, K. A. Abboud, and G. Christou, “Single-molecule magnets: A mn25 complex with a record  $s = 51/2$  spin for a molecular species,” *Journal of the American Chemical Society* **126**, 4766–4767 (2004), pMID: 15080666, <https://doi.org/10.1021/ja0316824>.
- <sup>28</sup>P. Abbasi, K. Quinn, D. I. Alexandropoulos, M. Damjanović, W. Wernsdorfer, A. Escuer, J. Mayans, M. Pilkington, and T. C. Stamatatos, “Transition metal single-molecule magnets: A Mn31 nanosized cluster with a large energy barrier of 60 k and magnetic hysteresis at 5 k,” *Journal of the American Chemical Society* **139**, 15644–15647 (2017), pMID: 29052991, <https://doi.org/10.1021/jacs.7b10130>.
- <sup>29</sup>A. J. Tasiopoulos, A. Vinslava, W. Wernsdorfer, K. A. Abboud, and G. Christou, “Giant single-molecule magnets: A Mn84 torus and its supramolecular nanotubes,” *Angewandte Chemie International Edition* **43**, 2117–2121 (2004), <https://onlinelibrary.wiley.com/doi/pdf/10.1002/anie.200353352>.

- <sup>30</sup>R. Hernández Sánchez and T. A. Betley, “Meta-atom behavior in clusters revealing large spin ground states,” *Journal of the American Chemical Society* **137**, 13949–13956 (2015), pMID: 26440452, <https://doi.org/10.1021/jacs.5b08962>.
- <sup>31</sup>C. Sangregorio, T. Ohm, C. Paulsen, R. Sessoli, and D. Gatteschi, “Quantum tunneling of the magnetization in an iron cluster nanomagnet,” *Phys. Rev. Lett.* **78**, 4645–4648 (1997).
- <sup>32</sup>A. K. Powell, S. L. Heath, D. Gatteschi, L. Pardi, R. Sessoli, G. Spina, F. Del Giallo, and F. Pieralli, “Synthesis, structures, and magnetic properties of fe<sub>2</sub>, fe<sub>17</sub>, and fe<sub>19</sub> oxo-bridged iron clusters: The stabilization of high ground state spins by cluster aggregates,” *Journal of the American Chemical Society* **117**, 2491–2502 (1995), <https://doi.org/10.1021/ja00114a012>.
- <sup>33</sup>C. Cadiou, M. Murrie, C. Paulsen, V. Villar, W. Wernsdorfer, and R. E. P. Winpenny, “Studies of a nickel-based single molecule magnet: resonant quantum tunnelling in an s = 12 molecule,” *Chem. Commun.* , 2666–2667 (2001).
- <sup>34</sup>M. Murrie, S. J. Teat, H. Stöckli-Evans, and H. U. Güdel, “Synthesis and characterization of a cobalt(ii) single-molecule magnet,” *Angewandte Chemie International Edition* **42**, 4653–4656 (2003), <https://onlinelibrary.wiley.com/doi/pdf/10.1002/anie.200351753>.
- <sup>35</sup>Y.-Z. Zhang, W. Wernsdorfer, F. Pan, Z.-M. Wang, and S. Gao, “An azido-bridged disc-like heptanuclear cobalt(ii) cluster: towards a single-molecule magnet,” *Chem. Commun.* , 3302–3304 (2006).
- <sup>36</sup>A.-L. Barra, P. Debrunner, D. Gatteschi, C. E. Schulz, and R. Sessoli, “Superparamagnetic-like behavior in an octanuclear iron cluster,” *Europhysics Letters (EPL)* **35**, 133–138 (1996).
- <sup>37</sup>O. Waldmann, “A criterion for the anisotropy barrier in single-molecule magnets,” *Inorganic Chemistry* **46**, 10035–10037 (2007), pMID: 17979271, <https://doi.org/10.1021/ic701365t>.
- <sup>38</sup>F. Neese and D. A. Pantazis, “What is not required to make a single molecule magnet,” *Faraday Discuss.* **148**, 229–238 (2011).
- <sup>39</sup>H. Oshio and M. Nakano, “High-spin molecules with magnetic anisotropy toward single-molecule magnets,” *Chemistry – A European Journal* **11**, 5178–5185 (2005), <https://chemistry-europe.onlinelibrary.wiley.com/doi/pdf/10.1002/chem.200401100>.
- <sup>40</sup>E. Ruiz, J. Cirera, J. Cano, S. Alvarez, C. Loose, and J. Kortus, “Can large magnetic anisotropy and high spin really coexist?” *Chem. Commun.* , 52–54 (2008).

- <sup>41</sup>L. M. C. Beltran and J. R. Long, "Directed assembly of metal-cyanide cluster magnets," *Accounts of Chemical Research* **38**, 325–334 (2005), pMID: 15835879, <https://doi.org/10.1021/ar040158e>.
- <sup>42</sup>X.-Y. Wang, C. Avendaño, and K. R. Dunbar, "Molecular magnetic materials based on 4d and 5d transition metals," *Chem. Soc. Rev.* **40**, 3213–3238 (2011).
- <sup>43</sup>K. S. Pedersen, J. Bendix, and R. Clérac, "Single-molecule magnet engineering: building-block approaches," *Chem. Commun.* **50**, 4396–4415 (2014).
- <sup>44</sup>D. N. Woodruff, R. E. P. Winpenny, and R. A. Layfield, "Lanthanide single-molecule magnets," *Chemical Reviews* **113**, 5110–5148 (2013), pMID: 23550940, <https://doi.org/10.1021/cr400018q>.
- <sup>45</sup>F.-S. Guo, A. K. Bar, and R. A. Layfield, "Main group chemistry at the interface with molecular magnetism," *Chemical Reviews* **119**, 8479–8505 (2019), pMID: 31059235, <https://doi.org/10.1021/acs.chemrev.9b00103>.
- <sup>46</sup>R. Sessoli and A. K. Powell, "Strategies towards single molecule magnets based on lanthanide ions," *Coordination Chemistry Reviews* **253**, 2328 – 2341 (2009), deutsche Forschungsgemeinschaft Molecular Magnetism Research Report.
- <sup>47</sup>S. G. McAdams, A.-M. Ariciu, A. K. Kostopoulos, J. P. Walsh, and F. Tuna, "Molecular single-ion magnets based on lanthanides and actinides: Design considerations and new advances in the context of quantum technologies," *Coordination Chemistry Reviews* **346**, 216 – 239 (2017), sI: 42 iccc, Brest– by invitation.
- <sup>48</sup>Z. Zhu, M. Guo, X.-L. Li, and J. Tang, "Molecular magnetism of lanthanide: Advances and perspectives," *Coordination Chemistry Reviews* **378**, 350 – 364 (2019), special issue on the 8th Chinese Coordination Chemistry Conference.
- <sup>49</sup>A. Dey, J. Acharya, and V. Chandrasekhar, "Heterometallic 3d–4f complexes as single-molecule magnets," *Chemistry – An Asian Journal* **14**, 4433–4453 (2019).
- <sup>50</sup>S. Demir, I.-R. Jeon, J. R. Long, and T. D. Harris, "Radical ligand-containing single-molecule magnets," *COORDINATION CHEMISTRY REVIEWS* **289**, 149–176 (2015).
- <sup>51</sup>R. A. Layfield, "Organometallic single-molecule magnets," *Organometallics* **33**, 1084–1099 (2014).
- <sup>52</sup>P. Hohenberg and W. Kohn, "Inhomogeneous electron gas," *Physical review* **136**, B864 (1964).
- <sup>53</sup>P. Hohenberg and W. Kohn, "Inhomogeneous electron gas," *Phys. Rev.* **136**, B864–B871

- (1964).
- <sup>54</sup>W. Kohn and L. J. Sham, “Self-consistent equations including exchange and correlation effects,” *Phys. Rev.* **140**, A1133–A1138 (1965).
- <sup>55</sup>J. C. Slater, “Wave functions in a periodic potential,” *Phys. Rev.* **51**, 846–851 (1937).
- <sup>56</sup>J. Slater, “Energy band calculations by the augmented plane wave method\*\*the research reported in this paper has been assisted by the national science foundation and the office of naval research, as well as by the army, navy, and air force.” (Academic Press, 1964) pp. 35–58.
- <sup>57</sup>O. K. Andersen, “Linear methods in band theory,” *Phys. Rev. B* **12**, 3060–3083 (1975).
- <sup>58</sup>D. D. Koelling and G. O. Arbman, “Use of energy derivative of the radial solution in an augmented plane wave method: application to copper,” *Journal of Physics F: Metal Physics* **5**, 2041–2054 (1975).
- <sup>59</sup>L. Zhang, A. Kozhevnikov, T. Schulthess, H.-P. Cheng, and S. B. Trickey, “Performance enhancement of apw+lo calculations by simplest separation of concerns,” *Computation* **10** (2022), 10.3390/computation10030043.
- <sup>60</sup>“Cuda toolkit documentation,” <https://docs.nvidia.com/cuda/index.html> (), version: v11.2.1.
- <sup>61</sup>N. M. Josuttis, *The C++ Standard Library: A Tutorial and Reference*, 3rd ed. (Addison-Wesley, Philadelphia, PA, 2000).
- <sup>62</sup>“Nvcc compiler,” <https://docs.nvidia.com/cuda/cuda-compiler-driver-nvcc/> ().
- <sup>63</sup>A. Kozhevnikov, A. G. Eguiluz, and T. C. Schulthess, “Toward first principles electronic structure simulations of excited states and strong correlations in nano- and materials science,” 2010 ACM/IEEE International Conference for High Performance Computing, Networking, Storage and Analysis , 1–10 (2010).
- <sup>64</sup>P. Blaha, H. Hofstätter, O. Koch, R. Laskowski, and K. Schwarz, “Iterative diagonalization in augmented plane wave based methods in electronic structure calculations,” *Journal of Computational Physics* **229**, 453–460 (2010).
- <sup>65</sup>A. Gulans, “Implementation of davidson iterative eigen solver for lapw,” to be published.
- <sup>66</sup>P. G. Sim and E. Sinn, “First manganese(iii) spin crossover, first d4 crossover. comment on cytochrome oxidase,” *Journal of the American Chemical Society* **103**, 241–243 (1981), <https://doi.org/10.1021/ja00391a067>.
- <sup>67</sup>J. P. Perdew, K. Burke, and M. Ernzerhof, “Generalized gradient approximation made

- simple,” *Phys. Rev. Lett.* **77**, 3865–3868 (1996).
- <sup>68</sup>G. Kresse and J. Furthmüller, “Efficient iterative schemes for ab initio total-energy calculations using a plane-wave basis set,” *Phys. Rev. B* **54**, 11169–11186 (1996).
- <sup>69</sup>S. Hill, R. S. Edwards, N. Aliaga-Alcalde, and G. Christou, “Quantum coherence in an exchange-coupled dimer of single-molecule magnets,” *Science* **302**, 1015–1018 (2003), <https://science.sciencemag.org/content/302/5647/1015.full.pdf>.
- <sup>70</sup>A. Wilson, S. Hill, R. S. Edwards, N. Aliaga-Alcalde, and G. Christou, “Entanglement of exchange-coupled dimers of single-molecule magnets,” *AIP Conference Proceedings* **850**, 1141–1142 (2006), <https://aip.scitation.org/doi/pdf/10.1063/1.2355106>.
- <sup>71</sup>R. Tiron, W. Wernsdorfer, D. Foguet-Albiol, N. Aliaga-Alcalde, and G. Christou, “Spin quantum tunneling via entangled states in a dimer of exchange-coupled single-molecule magnets,” *Phys. Rev. Lett.* **91**, 227203 (2003).
- <sup>72</sup>T. N. Nguyen, W. Wernsdorfer, K. A. Abboud, and G. Christou, “A supramolecular aggregate of four exchange-biased single-molecule magnets,” *Journal of the American Chemical Society* **133**, 20688–20691 (2011), PMID: 22136491, <https://doi.org/10.1021/ja2087344>.
- <sup>73</sup>T. N. Nguyen, M. Shiddiq, T. Ghosh, K. A. Abboud, S. Hill, and G. Christou, “Covalently linked dimer of mn3 single-molecule magnets and retention of its structure and quantum properties in solution,” *Journal of the American Chemical Society* **137**, 7160–7168 (2015), PMID: 26027646, <https://doi.org/10.1021/jacs.5b02677>.
- <sup>74</sup>V. S. Zapf, D. Zocco, B. R. Hansen, M. Jaime, N. Harrison, C. D. Batista, M. Kenzelmann, C. Niedermayer, A. Lacerda, and A. Paduan-Filho, “Bose-einstein condensation of  $s = 1$  nickel spin degrees of freedom in  $\text{NiCl}_2-4\text{SC}(\text{NH}_2)_2$ ,” *Phys. Rev. Lett.* **96**, 077204 (2006).
- <sup>75</sup>S. A. Zvyagin, J. Wosnitza, C. D. Batista, M. Tsukamoto, N. Kawashima, J. Krzystek, V. S. Zapf, M. Jaime, N. F. Oliveira, and A. Paduan-Filho, “Magnetic excitations in the spin-1 anisotropic heisenberg antiferromagnetic chain system  $\text{NiCl}_2-4\text{SC}(\text{NH}_2)_2$ ,” *Phys. Rev. Lett.* **98**, 047205 (2007).
- <sup>76</sup>V. S. Zapf, P. Sengupta, C. D. Batista, F. Nasreen, F. Wolff-Fabris, and A. Paduan-Filho, “Magnetoelectric effects in an organometallic quantum magnet,” *Phys. Rev. B* **83**, 140405 (2011).
- <sup>77</sup>V. S. Zapf, V. F. Correa, P. Sengupta, C. D. Batista, M. Tsukamoto, N. Kawashima, P. Egan, C. Pantea, A. Migliori, J. B. Betts, M. Jaime, and A. Paduan-Filho, “Direct measurement of spin correlations using magnetostriction,” *Phys. Rev. B* **77**, 020404 (2008).

- <sup>78</sup>R. Yu, L. Yin, N. S. Sullivan, J. Xia, C. Huan, A. Paduan-Filho, N. F. Oliveira, S. H. Jr, A. Steppke, C. F. Miclea, F. Weickert, R. Movshovich, E.-D. Mun, B. L. Scott, V. S. Zapf, and T. Roscilde, “Bose glass and mott glass of quasiparticles in a doped quantum magnet,” *Nature* **489**, 379 (2012).
- <sup>79</sup>M. Yazback, J.-X. Yu, S. Liu, L. Zhang, N. S. Sullivan, and H.-P. Cheng, “First-principles study of an  $s = 1$  quasi one-dimensional quantum molecular magnetic material,” *Phys. Rev. B* **103**, 054434 (2021).
- <sup>80</sup>A. I. Johnson, F. Islam, C. M. Canali, and M. R. Pederson, “A multiferroic molecular magnetic qubit,” *The Journal of Chemical Physics* **151**, 174105 (2019), <https://doi.org/10.1063/1.5127956>.
- <sup>81</sup>M. Gakiya Teruya, X. Jiang, D. Le, O. Ungor, A. J. Durrani, J. J. Koptur Palenchar, J. Jiang, T. Jiang, M. W. Meisel, H.-P. Cheng, X.-G. Zhang, X.-X. Zhang, T. S. Rahman, A. F. Hebard, and M. Shatruk, “Asymmetric design of spin crossover complexes to increase the volatility for surface deposition,” *Journal of the American Chemical Society* **143**, 14563–14572 (2021).
- <sup>82</sup>D. Le, T. Jiang, M. Gakiya-Teruya, M. Shatruk, and T. S. Rahman, “On stabilizing spin crossover molecule [fe(tBu2qsal)2] on suitable supports: insights from ab initio studies,” *Journal of Physics: Condensed Matter* **33**, 385201 (2021).